1 **High-density transposon mutagenesis in *Mycobacterium abscessus* identifies an**

2 **essential penicillin-binding lipo-protein (PBP-lipo) involved in septal peptidoglycan**

3 **synthesis and antibiotic sensitivity**

4

5 **Chidiebere Akusobi[1], Bouchra S. Benghomari[2], Ian D. Wolf[1], Shreya Singhvi[3], Junhao**
6 **Zhu[1], Charles L. Dulberger[1], Thomas R. Ioerger[4], Eric J. Rubin[1]**
7
8
9 [1]Department of Immunology and Infectious Diseases, Harvard T.H. Chan School of Public
10 Health, Boston, MA 02115, USA

11
12 [2]Department of Biology, Northeastern University, Boston, MA 02115, USA

13 [3]Department of Molecular and Cell Biology, University of California, Berkeley, Berkeley, CA

14 94720, USA

15 [4]Department of Computer Science and Engineering, Texas A&M University, College Station
16 Texas 77843, USA

Abstract

Mycobacterium abscessus (*Mab*) is a rapidly growing non-tuberculous mycobacterium (NTM) that causes a wide range of infections. Treatment of *Mab* infections is difficult because the bacterium is intrinsically resistant to many classes of antibiotics. Developing new and effective treatments against *Mab* requires a better understanding of the unique vulnerabilities that can be targeted for future drug development. To achieve this, we identified essential genes in *Mab* by conducting transposon-sequencing (TnSeq) on the reference *Mab* strain ATCC 19977. We generated ~51,000 unique transposon mutants and used this high-density library to identify 362 essential genes for *in vitro* growth. To investigate species-specific vulnerabilities in *Mab*, we further characterized *MAB_3167c*, a predicted penicillin-binding-lipoprotein (PBP-lipo) that is essential in *Mab* and non-essential in *M. tuberculosis* (*Mtb*). We found that PBP-lipo primarily localizes to the subpolar region and later to the septum as cells prepare to divide. Knockdown of *Mab* PBP-lipo causes cells to elongate, develop ectopic branches, and form multiple septa. Dual knockdown of PBP-lipo with PBPs, PbpB, DacB1, and a carboxypeptidase, MAB_0519 lead to synergistic growth arrest. In contrast, these genetic interactions were absent in the *Mtb* model organism, *M. smegmatis*, indicating that the PBP-lipo homologs in the two species exist in distinct genetic networks. Finally, repressing PBP-lipo sensitized the reference strain and 11 *Mab* clinical isolates to several classes of antibiotics, including the β-lactams, ampicillin and amoxicillin by greater than 128-fold. Altogether, this study presents PBP-lipo as a key enzyme to study *Mab* specific processes in cell wall synthesis and importantly positions PBP-lipo as an attractive drug target to treat *Mab* infections.

Introduction

Mycobacterium abscessus (*Mab*) is the most common cause of human disease among the rapidly growing non-tuberculous mycobacteria (NTM). It causes a wide range of illnesses including lung, skin and soft-tissue infections, as well as disseminated disease (1–3). While the incidence of *Mab* infections is rising worldwide, treating *Mab* infections remains difficult. The bacterium has intrinsic and acquired resistance mechanisms to many classes of antibiotics, including the standard drugs used to treat tuberculosis (4,5). The current treatment regimen for *Mab* requires taking a combination of multiple antibiotics for up to 18 months and is often associated with severe toxicity and routinely ends in treatment failure (6). Thus, there is an urgent need for new and effective drugs to treat the emerging global public health threat of *Mab* infections (7).

Developing novel antibiotic treatments for *Mab* requires a better understanding of essential biological processes in the bacterium that can be targeted. Identifying essential genes is the first step in this process, and by combining transposon-mutagenesis with massive parallel sequencing, transposon-sequencing (TnSeq) has been an effective tool to determine gene essentiality on a genome-wide scale in other microbes (8). However, while many TnSeq screens have been conducted in *M. tuberculosis* (*Mtb*) (9), up until recently only 2 published TnSeq screens have been reported in *Mab* (10,11). While both *Mab* TnSeq screens have provided tools and important insights into *Mab* biology, neither utilized a mutant library with high enough density to comprehensively identify essential genes. This changed with the recent publication from Rifat *et al*, who generated robust high-density transposon libraries of *Mab* and identified a comprehensive list of genetic elements essential for *in vitro* growth (12). Identification of these essential genes serves as an excellent starting point to classify attractive targets for drug discovery.

3

67   One major target of antibiotics is the mycobacterial cell wall whose biogenesis is essential for

68   bacterial growth (13,14). The structure of the mycobacterial cell wall is unique among bacteria

69   because it is composed of three macromolecules: peptidoglycan (PG), arabinogalactan, and

70   mycolic acids. Together, these layers envelop mycobacteria with a thick, waxy coat that forms a

71   permeability barrier to many drugs (15,16). The foundational layer is comprised of peptidoglycan

72   (PG), which consists of glycan sugars cross-linked by short peptides forming a continuous, net-

73   like structure that maintains cell shape and prevents rupture. Mycobacteria build new PG at the

74   cell poles aided by Class A penicillin binding proteins (PBPs) that perform two reactions: a

75   transglycosylation reaction that polymerizes PG monomers to existing glycan strands and a

76   transpeptidation reaction that cross-links glycan strands to each other (17). Class B PBPs solely

77   perform the cross-linking reactions (18,19). A hallmark of PBPs is that they are inhibited by β-

78   lactam antibiotics; however, these antibiotics are typically not used to treat *Mab* infections due

79   to high levels of resistance and the presence of β-lactamases in the genome (20).

80

81   To identify essential genes for *in vitro* growth and classify potential new drug targets in *Mab*, we

82   performed TnSeq. We generated high-density transposon libraries of ~51,000 mutants in the

83   reference strain, *M. abscessus subsp. abscessus* ATCC 19977 and identified 362 genes

84   required for *in vitro* growth. We next identified essential genes in *Mab* that were non-essential in

85   *Mtb* in order to study species-specific vulnerabilities in *Mab*. From this list of genes, we further

86   characterized *MAB_3167c*, which encodes PBP-lipo, a conserved Class B PBP. We found that

87   PBP-lipo is required for normal peptidoglycan (PG) synthesis, cell division, and sensitizes *Mab*

88   to commonly-used β-lactams and other classes of antibiotics. None of these phenotypes were

89   present in the *Msm* and *Mtb* PBP-lipo knockouts. Thus, we find that PBP-lipo has a unique

90   essential function in *Mab* and is a potential drug target for treating *Mab* infections.

Results

Identification of *M. abscessus* ATCC 19977 essential genes for *in vitro* growth

To identify essential genes in *Mab*, we performed TnSeq on *M. abscessus subsp. abscessus* ATCC 19977 (hereafter referred to as *Mab*) using the φMycoMar T7 phage carrying the Himar1 transposon for transduction. This transposon inserts into 'TA' dinucleotide sites and disrupts gene function (Figure 1A) (21). We transduced three independently grown cultures of *Mab*, yielding triplicate libraries with saturations of 54.2%, 62.3%, and 64.1% for Library 1, 2, and 3 respectively (Supplemental Table 1). The average Pearson r^2 correlation of mean read counts for each gene across 2 libraries was 0.85 indicating good correlation among the libraries (Supplemental Figure 1). The transposon insertions across the three libraries were mapped onto the *Mab* genome as depicted in the chromosome map (Figure 1B). Across three libraries, we generated approximately 51,000 unique transposon mutants, as defined by sites of unique transposon insertions across all three libraries. Of note, the *Mab* libraries shared the same non-permissive 'TA' sites for transposon insertion as has been described in other mycobacterial species (Shoudhery *et al*, bioRxiv 2021).

The high density of these libraries allowed us to identify essential *Mab* genes using the Hidden Markov Model (HMM) algorithm implemented by TRANSIT (22). HMM identified 362 genes as essential, 4167 as non-essential, 153 as producing growth defect when disrupted, and 233 as causing a growth advantage when disrupted (Figure 1C, Supplemental Table 2). As expected, many of the genes identified as essential were involved in key biological processes including protein translation, amino acid metabolism, and cell wall biogenesis based on Clusters of Orthologous Groups (COG) analysis (Figure 1E).

Identification and Validation of uniquely essential genes in *Mab*

5

117   Understanding differences in essential genes between *Mab* and *Mtb* might uncover new ways of

118   specifically targeting *Mab*. Thus, we identified *Mab*-specific essential genes by comparing gene

119   essentiality between mutual orthologs of *Mab* and *Mtb*. We used *Mtb* essentiality data

120   generated from a comprehensive analysis on *Mtb* essentiality using 14 high-quality TnSeq

121   datasets (9). Of the 2279 mutual orthologs between *Mab* and *Mtb*, 282 genes were essential in

122   both species. We focused on the mutual orthologs that that were essential in *Mab,* but non-

123   essential in *Mtb*. These genes could potentially represent *Mab* specific drug targets. Exactly 20

124   genes fit into this category, which we refer to as "uniquely essential" (Figure 1D) (Supplemental

125   Table 3).

126

127   To understand the quality of predictions by TnSeq, we validated the essentiality of a subset of

128   genes using an anhydrotetracycline (ATc) inducible CRISPRi system developed for use in *Mtb*

129   (23). Expression of a non-targeting sgRNA control in this system has no impact on cell

130   proliferation (Figure 2A). In contrast, repressing canonical essential genes *rpoB, gyrB,* and *secY*

131   impaired cell growth in both liquid broth (Figure 2A) and solid media (Supplemental Figure 2A),

132   indicating that the CRISPRi system developed in *Mtb* functions in *Mab*.

133

134   We next validated the essentiality of a subset of the 20 uniquely essential genes in *Mab*: *glnA2,*

135   *icd2, sdhA,* and *MAB_4471*. CRISPRi knockdown of these uniquely essential genes impaired

136   growth in liquid media (Figure 2B) as well as solid media (Supplemental Figure 2B). These

137   results confirm that at least a subset of uniquely essential *Mab* genes identified by TnSeq are

138   required for optimal *in vitro* growth. The slight rise in OD_{600} later in the time course is consistent

139   with the emergence of escape mutants in the CRISPRi system, which has been previously

140   described (24,25).

141

142   **PBP-lipo is uniquely essential in *Mab***

143   One of the uniquely essential genes we identified was *MAB_3167c*, which encodes a Class B

144   penicillin-binding lipoprotein (PBP-lipo). PBP-lipo is predicted to have a single N-terminal

145   transmembrane helix and a transpeptidase domain. From our *Mab* TnSeq data, *MAB_3167c*

146   lacked transposon insertions across all three replicate libraries (Figure 3A). This finding

147   corroborates data from previously generated *Mab* transposon libraries that show lack of

148   insertions in *MAB_3167c* (10,12). Comparing the essentiality of PBP enzymes in *Mab* with their

149   homologs in *Mtb* revealed that *pbp-lipo* is unique in being the sole PBP whose essentiality

150   differs between the two species. Specifically, *pbp-lipo* is essential in *Mab* and non-essential in

151   *Mtb in vitro* (Figure 3B).

152

153   To validate that PBP-lipo is required for *in vitro* growth, we used the CRISPRi system to induce

154   knockdown using constructs encoding 1, 2, or 3 sgRNAs targeting *pbp-lipo* (Supplemental

155   Figure 3A). The single, double, or triple sgRNA constructs allowed for the fine tuning of the

156   magnitude of *pbp-lipo* knockdown, as measured by RT-qPCR (Supplemental Figure 3B). We

157   noted that the empty vector control (0 sgRNA) and single sgRNA construct had no detectable

158   effect on the growth of *Mab* (Supplemental Figure 3C). In contrast, when *pbp-lipo* was targeted

159   with either 2 or 3 sgRNAs, the growth of *Mab* was inhibited, indicating that *pbp-lipo* is indeed

160   required for optimal *in vitro* growth (Figure 3C). We also observed the inhibition of cell growth on

161   solid media where knockdown of PBP-lipo by 2 sgRNA and 3 sgRNA vectors led to a 1000-fold

162   reduction in colony forming units (CFU) (Supplemental Figure 3D). To complement the PBP-lipo

163   knockdown growth defect phenotype, we recoded a version of PBP-lipo with the protospacer

164   adjacent motif (PAM) sequence mutated. This prevents sgRNAs from binding the introduced

165   PBP-lipo copy present on the integrated plasmid. When constitutively expressed, this recoded

166   PBP-lipo rescued growth of the native PBP-lipo knockdown (Supplemental Figure 3D). In

167   contrast, a recoded and catalytically-dead mutant of PBP-lipo did not rescue growth. This data

168   demonstrates that PBP-lipo's transpeptidase activity is required for *Mab* optimal growth.

7

169

170   In contrast to *Mab*, when we deleted the gene encoding PBP-lipo in *Mtb*, *Rv2864c*, the growth

171   of the knockout and wild-type strains was indistinguishable (Figure 3D). Similarly, the PBP-lipo

172   homolog in *Msm, MSMEG_2584c*, when knocked out grew identically to wildtype with no growth

173   defect (Supplemental Figure 4). Taken together, these data demonstrate that PBP-lipo is

174   essential for growth in *Mab,* while its homologs in *Mtb* and *Msm* are non-essential.

175

176   **PBP-lipo is required to maintain normal cell elongation and division**

177   A hallmark of PBPs is that they bind β-lactam antibiotics. Therefore, to test whether PBP-lipo is

178   an active PBP in *Mab*, we determined whether PBP-lipo binds bocillin FL, a fluorescent analog

179   of penicillin (26). Using a strain that constitutively expresses a strep-tagged PBP-lipo, we

180   identified a fluorescent bocillin FL band at the same molecular weight as PBP-lipo, which was

181   confirmed to be PBP-lipo by Western blot (Supplemental Figure 5). These data suggest that

182   PBP-lipo binds bocillin FL *in vivo* and is an active PBP. Interestingly, in wildtype *Mab,* we did not

183   detect an obvious PBP-lipo band at the predicted molecular weight of PBP-lipo, 63 kDa,

184   suggesting that native expression levels of PBP-lipo is either low or PBP-lipo is expressed at

185   distinct times during the cell cycle.

186

187   In mycobacteria, the PG layer is critical for maintaining normal cell shape and altering PBP

188   expression often results in abnormal cell morphology. Thus, we studied the morphology of *Mab*

189   when PBP-lipo was repressed and discovered dramatic morphological changes. *Mab* cells

190   elongate, branch inappropriately, and form ectopic poles of active growth, as evidenced by

191   staining with NADA, a fluorescent-D-amino acid (FDAA) that binds areas of active PG synthesis

192   (27) (Figure 4A). PBP-lipo knockdown significantly increased the number of cells with ectopic

193   branches (Supplemental Figure 6B). Furthermore, during normal growth of *Mab*, a small

194   percentage of cells contain one mid-cell FDAA band, indicating active PG synthesis at the site

195   of septation. However, when PBP-lipo is knocked down, we occasionally find cells with 2 or 3

196   bands mid-cell, as exemplified in the 2 sgRNA + panel (Figure 4A). PBP-lipo knockdown strains

197   were all significantly longer than their uninduced controls, with the longest average cell length

198   belonging to the strain with the strongest PBP-lipo knockdown (Figure 4B). Of note, while the 0

199   sgRNA +/- cells are by eye morphologically indistinguishable, there is a statistically significant

200   difference in the mean cell lengths, likely due to the effect of ATc on cells (Figure 4B). Notably,

201   cell width did not change among the strains (Supplemental Figure 6A). In comparison, in *Msm*

202   and *Mtb*, there were no differences in morphology and cell length between the wildtype and

203   PBP-lipo knockout strains (Supplemental Figure 7). The dramatic changes in *Mab* morphology

204   when PBP-lipo is repressed suggests proper expression of this enzyme is required for

205   maintaining normal *Mab* elongation and division.

206

207   **PBP-lipo localizes to the subpolar regions and to the mid-cell before cell division**

208   The morphological defects caused by PBP-lipo knockdown were reminiscent of septal factor

209   depletions observed in *Msm* (28). Thus, we hypothesized that PBP-lipo localizes to the septum.

210   To test this hypothesis, we N-terminally tagged PBP-lipo with mRFP, which has been previously

211   shown to function in the mycobacterial periplasm (29). This mRFP-PBP-lipo construct was

212   constitutively expressed and visualized with fluorescence microscopy. We discovered that PBP-

213   lipo localized to the subpolar regions of the cell and the mid-cell, likely in the growing septum

214   (Figure 5A). The resulting microscopy images were analyzed using OMEGA, which quantified

215   the fluorescent signal across the cell normalized by cell length (Zhu *et al*, unpublished). We then

216   binned the cells into quartiles according to their length and found that the mRFP-PBP-lipo

217   fluorescent signal was concentrated at the sub-polar regions for cells of all lengths, while the

218   mid-cell localization of PBP-lipo was only present in the longest cells in the population (Figure

219   5B). These data suggest that as cells elongate, PBP-lipo localizes to the septum and is likely

220   involved in septum formation and cell division.

221

PBP-lipo is incorporated into a unique PG network in *Mab* that does not exist in *Msm*

223   Given that *Mtb* and *Msm* do not have duplicates of PBP-lipo in their genomes, we hypothesized

224   other reasons for the differential essentiality of PBP-lipo between these species. It is possible

225   that there is a functional difference between PBP-lipo in *Mab* and its homologs in *Msm* and *Mtb*.

226   This possibility intrigued us because an alignment of PBP-lipo from various mycobacteria

227   revealed that PBP-lipo$_{Mab}$ has 5 additional amino acids present only in the *Mab* homolog

228   (Supplemental Figure 8A). When *in silico* structures of PBP-lipo$_{Mab}$ and PBP-lipo$_{Mtb}$ are

229   modeled, these 5 extra residues form an appendage we hypothesized could impart PBP-lipo$_{Mab}$

230   with additional ability to bind proteins (Supplemental Figure 8B).

231

232   To test this hypothesis, we constitutively expressed PBP-lipo$_{Msm}$ in the 2 sgRNA *Mab* strain

233   (hereafter referred to as the *Msm* complement strain). As expected, knockdown of the native

234   *Mab* PBP-lipo impairs growth. However, PBP-lipo$_{Msm}$ expression in the 2 sgRNA strain rescued

235   *Mab* growth (Figure 6A). Furthermore, expressing PBP-lipo$_{Msm}$ eliminated the branching

236   phenotype of the native PBP-lipo knockdown and partially reversed the elongated phenotype as

237   well (Figure 6B). The recoded version of PBP-lipo$_{Mab}$ also reversed the branching of cells and

238   partially complemented the elongated phenotype (Figure 6B). In contrast, the catalytically-dead

239   version of PBP-lipo$_{Mab}$-(S364A) did not complement, with cells appearing elongated and

240   branched (Figure 6B, Supplemental Figure 9). These results demonstrate that PBP-lipo$_{Msm}$ can

241   rescue knockdown of the endogenous *Mab* enzyme. From these data, we conclude that the

242   essentiality of PBP-lipo$_{Mab}$ is not solely due to a unique functional property that is present only in

243   the *Mab* homolog.

244

245   An alternative hypothesis is PBP-lipo participates in a PBP interaction network in *Mab* that is

246   distinct from respective PBP networks in *Msm* and *Mtb*. In short, while PBP-lipo is required in

10

247   the *Mab* PBP network*,* its function is likely redundant in the networks of *Msm* and *Mtb.* This

248   notion of functionally distinct PBP networks has been previously described in mycobacteria (30).

249   To interrogate the PBP network of *Mab*, we tested which PBPs genetically interacted with PBP-

250   lipo. To perform this experiment, we cloned CRISPRi constructs with sgRNAs that would weakly

251   knockdown each PBP in *Mab* (PBPx) so that growth was not significantly impaired. We also

252   cloned combinatorial CRISPRi constructs where PBP-lipo and another PBP were weakly

253   repressed. Using this dual sgRNA vector, we could simultaneously knockdown PBP-lipo and a

254   PBP of interest.

255

256   Using combinatorial knockdowns of each PBP, we compared growth inhibition when a single

257   PBP was knocked down versus when PBP-lipo and a second PBP were jointly repressed. Of

258   the 8 combinations we tested, we found that knockdown of three PBPs with PBP-lipo lead to

259   synergistic growth arrest (Figure 6C). These enzymes were *pbpB, dacB1,* and *MAB_0519,*

260   which encodes a protein with a hypothesized carboxypeptidase domain. This genetic synergy

261   was also observed in liquid culture for *pbpB* and *dacB1* (Supplemental Figure 10A). The

262   homolog of PbpB is a well-studied enzyme in both *Msm, Mtb,* and the model organisms *E. coli*

263   and *B. subtilis,* where it is known as FtsI*.* In all these organisms, PbpB localizes to the septum

264   and is largely responsible for septal PG synthesis (31–33). Interestingly, like PbpB and PBP-

265   lipo, we found DacB1 localizes to the septum (Supplemental Figure 10B). These data suggest

266   that PBP-lipo genetically interacts with PbpB and DacB1, and that all three enzymes localize to

267   the same region of the cell and could potentially coordinate septal PG synthesis in a complex

268   together.

269

270   We next tested whether the same PBP-lipo genetic interactions existed in *Msm.* We used

271   CRISPRi to knockdown *Msm* PBP homologs in the wildtype *Msm* and the *pbp-lipo* knockout

272   background. In this experiment, genes that interacted with PBP-lipo would show impaired cell

273   growth when repressed in the PBP-lipo knockout. Interestingly, we did not observe genetic

274   interactions between any of the PBPs tested and PBP-lipo (Figure 6D). This was true for the

275   PBPs tested with homologs in *Mab* and additional PBPs present in the *Msm* genome

276   (Supplemental Figure 11).

277

278   We next used a whole genome approach to identify genes in *Msm* that genetically interact with

279   PBP-lipo. We generated high density transposon mutant libraries in both the wildtype and PBP-

280   lipo knockout strains of *Msm* to identify genes that were conditionally essential in the knockout

281   background. The saturation of the 2 wildtype libraries were 51.9% and 53.4%, while the

282   saturation of the PBP-lipo knockout library was 62.4%. Using the resampling method in

283   TRANSIT, our TnSeq data revealed that there were no conditionally essential genes in the

284   ΔPBP-lipo *Msm* background (Supplemental Table 4). These data strongly suggest PBP-lipo in

285   *Msm* exists in a robust genetic network with multiple functional redundancies. To uncover PBP-

286   lipo's function in *Msm*, it is possible that double and triple knockout mutants of PG synthesis

287   enzymes would need to be generated.

288

289   **Repressing PBP-lipo sensitizes *Mab* to a wide range of antibiotics**

290   Given PBP-lipo's essentiality in *Mab* and the genetic interactions it has with other PBPs, we

291   hypothesized that repressing PBP-lipo would affect *Mab*'s sensitivity to antibiotics, including β-

292   lactams. To test this hypothesis, we measured the sensitivity of PBP-lipo knockdown cells to 21

293   antibiotics that target translation, transcription, and DNA replication in both *Mab* and *Msm*.

294

295   Wildtype *Mab* is typically resistant to β-lactams amoxicillin and ampicillin with MICs greater than

296   >256 µg/ml. When PBP-lipo is knocked down, the MIC for both antibiotics dropped to 2 µg/ml,

297   indicating a greater than 128-fold sensitization (Table 1). These results indicate a strong

298   chemical-genetic interaction between PBP-lipo and both ampicillin and amoxicillin. Interestingly,

299   not all β-lactams had shifts in their MIC when PBP-lipo was knocked down. This indicates that

300   there is a specific chemical-genetic interaction between PBP-lipo and ampicillin and amoxicillin.

301   MIC changes for other β-lactams were less drastic, with a 4-8- fold reduction observed for

302   faropenem and cefoxitin (Table 1). PBP-lipo knockdown also affects susceptibility to antibiotics

303   that do not target the cell wall. The macrolides, clarithromycin and erythromycin, were 128-fold

304   and 64-fold more potent respectively in the PBP-lipo knock down cells. A 16-fold reduction in

305   MIC was observed for RNA polymerase inhibitor, rifampicin.

306

307   The MIC differences in rifampicin and clarithromycin are notable because these antibiotics do

308   not target the cell wall. Thus, the mechanism of synergy between PBP-lipo repression and these

309   antibiotics likely differs from the synergy with ampicillin and amoxicillin. We posited that PBP-

310   lipo repression might increase the permeability of the cell wall, allowing more drug to enter the

311   cell. To test this hypothesis, we measured the accumulation of calcein into *Mab*, which is proxy

312   for cell permeability. Calcein accumulates more rapidly in PBP-lipo knockdown cells, indicating

313   that PBP-lipo increases the permeability of *Mab* cells (Supplemental Figure 13). This increased

314   permeability likely leads to increased antibiotic access to the cell, thus sensitizing the bacteria to

315   the antibiotics.

316

317   When the MICs of the same 21 antibiotics tested in *Mab* were measured in the PBP-lipo

318   knockout in *Msm,* we observed no difference in the MICs (Supplemental Table 5). We also

319   measured the MICs of a subsection of these antibiotics in the *pbp-lipo* knockout in *Mtb* and

320   found no difference in MICs between the wildtype and knockout strain (Supplemental Table 6).

321   These data suggest that PBP-lipo's unique function in *Mab's* PG synthesis network likely

322   contributes to the bacterium's sensitivity to antibiotics when the enzyme is repressed.

323

Repression of PBP-lipo sensitizes *Mab* clinical isolates to antibiotics

324

325 The antibiotic experiments were conducted on the ATCC 19977 reference strain on *Mab*, which

326 is lab adapted, after being isolated from a knee abscess in the 1950s and propagated in the lab

327 since (3,34). Work performed in *Mtb* has demonstrated clinical isolates and lab-adapted strains

328 respond to antibiotics stressors differently (35). As a result, we tested whether knockdown of

329 PBP-lipo in *Mab* clinical isolates led to the same changes in antibiotic sensitivity as observed in

330 the reference strain.

331

332 We found that knockdown of PBP-lipo using the 3 sgRNA construct impaired cell growth in all

333 11 clinical isolates leading to a 100 to 10,000-fold difference in CFUs (Supplemental Figure

334 12A). We also confirmed in a sub-set of the clinical isolates that PBP-lipo knockdown lead to

335 elongated and inappropriately branched cells, as observed in the reference strain

336 (Supplemental Figure 12B). After confirming the PBP-lipo phenotypes in the clinical isolates, we

337 measured the MICs of ampicillin, amoxicillin, meropenem, rifampicin, and clarithromycin on *pbp-*

338 *lipo* knockdowns of the clinical isolates.

339

340 For amoxicillin and ampicillin, PBP-lipo knockdown reduced the MICs by >32 to >512-fold.

341 Meropenem served as a negative control and indeed, there was no difference in MICs between

342 uninduced and induced strains (Table 2). Finally, we observed an >8X-32X fold difference in the

343 MICs for rifampicin and 8 to 128-fold difference in the MICs for clarithromycin (Table 3).

344 Altogether, the antibiotic sensitivity data demonstrate that the phenotypic consequences of

345 repressing PBP-lipo is not only limited to the lab-adapted reference strain, but is also observed

346 in *Mab* clinical isolates.

Discussion

347

348   Developing new drugs and drug regimens against *Mab* requires a better understanding of the

349   bacterium's essential processes. This includes identifying essential *Mab* genes for further

350   characterization as potential drug targets. To do this, we generated high-density transposon

351   libraries to identify essential genes in the reference strain, *M. abscessus subsp. abscessus*

352   ATCC 19977*.* Importantly, *Mab* transposon libraries with fewer than 10,000 unique mutants

353   have been previously published, but these studies did not fully identify the list of essential genes

354   in *Mab* (10,11). Recently, Rifat *et al* successfully generated high-density libraries and were the

355   first group to identify essential genes and genomic elements in the *Mab* genome (12). All

356   together, they identified 326 essential genes and compared this list to essential genes identified

357   in *Mtb* and *Mycobacterium avium.* Similar to our study, Rifat *et al* highlighted uniquely essential

358   genes in *Mab,* which they also state deserve further study as these genes could represent *Mab*

359   specific drug targets (12).

360

361   In addition to identifying essential genes in *Mab*, our study builds off of Rifat *et al's* work by

362   using CRISPRi to efficiently repress gene expression and validate predicted essential genes as

363   required for *in vitro* growth (23). Furthermore, we found that by targeting genes with multiple

364   sgRNAs, CRISPRi can achieve significant gene repression, allowing for the investigation of

365   essential genes and providing an alternative to gene knockouts. Constructing gene knockouts in

366   *Mab* can be inefficient (36); thus, CRISPRi provides a convenient tool for genetic manipulation

367   in *Mab.* Overall, the newly generated *Mab* transposon libraries can be used to determine genes

368   required for growth in a variety of conditions including infection models, biofilms, and antibiotic

369   stress.

370

371   Both Rifat *et al's* and our TnSeq data identified PBP-lipo as the sole peptidoglycan synthesis

372   gene that was essential in *Mab* and non-essential in *Mtb* (12)*.* Using CRISPRi, we

15

373   demonstrated the necessity of PBP-lipo expression for *Mab* to maintain normal morphology and

374   to divide properly. When PBP-lipo is repressed, cells elongate, branch, and form ectopic poles.

375   We localized PBP-lipo to the subpolar regions of the cell, and as cells elongate and prepare for

376   division, PBP-lipo localizes to the septum. This constellation of phenotypes mimic septal-factor

377   depletions observed in *Msm,* which also causes cells to elongate, branch, and form ectopic

378   poles (28). These data suggest that PBP-lipo is involved with PG synthesis at the septum and

379   that depletion of the enzyme likely leads to dysregulated septal PG synthesis and aberrant cell

380   division.

381

382   Given PBP-lipo's localization and effect on cell division, we posit PBP-lipo acts as an essential

383   septal PG synthesis enzyme in *Mab.* In *Mtb* and *Msm,* this is accomplished by the enzyme

384   *pbpB*, which is essential for growth. Additionally, when *pbpB* is repressed in these species, cells

385   appear morphologically similar to the PBP-lipo knockdown in *Mab* (28,31). Interestingly, PBP-

386   lipo knockouts in both *Msm* and *Mtb* are morphologically identical to wildtype cells

387   (Supplemental Figure 7). These data underscore the notion that biological insights from *Msm*

388   and *Mtb* should not be de-facto applied to *Mab*. We hypothesize that PBP-lipo is a member of

389   the *Mab* divisome complex, a collection of structural proteins and enzymes that coordinates cell

390   division (37). Future studies are needed to determine if PBP-lipo interacts with known septal

391   factors, such as FtsQ, FtsW, FtsZ, whose functions have been described in *Msm* (38–40).

392   Future work may also reveal novel PBP-lipo binding factors that coordinate PG synthesis and

393   cell division in *Mab*.

394

395   Phenotypes characteristic of the PBP-lipo knockdown in *Mab* were absent in the *Mtb* and *Msm*

396   PBP-lipo knockouts. Both *Mtb* and *Msm* do not have a duplicate copy of PBP-lipo in their

397   genomes. Thus, to explain the differential essentiality of PBP-lipo across these mycobacterial

398   species, one hypothesis we explored was differences in the genetic networks of PG synthesis

399   enzymes. Construction of the PG layer is a complex process that involves a collection of

400   enzymes that work in concert to ensure proper synthesis and remodeling. Previous work has

401   shown that PG synthesis enzymes belong to genetic and spatiotemporal networks that do not

402   necessarily replicate across closely related species (30,41). Thus, while the building blocks to

403   construct the PG layer may be similar between species, how the enzymes are networked and

404   subsequently function together may differ. We demonstrated that PBP-lipo genetically interacts

405   with *pbpB, dacB1,* and *MAB_0519*. In contrast, TnSeq of the *Msm* Δ*pbp-lipo* strain did not

406   reveal interactions with any other gene in the genome. The TnSeq data demonstrates that

407   despite being homologs, PBP-lipo in *Mab* and *Msm* are incorporated into different PG synthesis

408   networks. In *Mab,* this network renders PBP-lipo's function as essential for growth, whereas in

409   *Msm,* PBP-lipo is dispensable. Interestingly, in *Mtb* PBP-lipo became more required in a *ponA2*

410   knockout suggesting that PBP-lipo and PonA2 genetically interact *Mtb* (30) – a genetic

411   interaction that was not observed in *Mab*. This observation supports the hypothesis that PBP-

412   lipo is incorporated in different PG synthesis in *Mtb* as well.

413

414   In *Mab,* the three genes that genetically interacted with PBP-lipo, *pbpB, dacB1,* and *MAB_0519,*

415   are all hypothesized to be septal associated. PbpB is a D,D-transpeptidase that performs 4,3

416   crosslinking reactions at the septum. In both *E. coli* and *Msm*, depleting PbpB leads to cell

417   elongation and branching, reminiscent of the *Mab* PBP-lipo knockdown phenotypes (28). A

418   potential explanation of this genetic interaction is both PbpB and PBP-lipo perform 4,3-

419   crosslinking at the *Mab* septum. In this model, repressing both enzymes would dramatically

420   reduce 4,3-crosslinking at the septum and lead to cell death. It is possible that PBP-lipo and

421   PbpB have overlapping 4-3 cross-linking function at the septum. However, given that PBP-lipo

422   and PbpB are essential in *Mab*, both enzymes must have distinct functional roles. Their distinct

423   functions could be revealed by identifying unique genetic interactions each enzyme has with

17

424   other PG synthesis enzymes. Why *Mab* would require two PG 4,3 crosslinking enzymes

425   functioning at the septum is an intriguing area of future research.

426

427   The two other genes that synergized with PBP-lipo, DacB1 and MAB_0519, are both

428   hypothesized carboxypeptidases that cleave the terminal D-ala-D-ala on the pentapeptide

429   chains of PG monomers (42,43). This reaction is necessary for the subsequent 4,3 crosslinks

430   catalyzed by D-D transpeptidases like PbpB and PBP-lipo. Interestingly, DacB1 localizes to the

431   septum in *Mab* and has been described as septally localized in *Msm* and *Mtb* (44)*.* Furthermore,

432   the homolog of MAB_0519 in *Mtb*, Rv3627c is involved in septal PG synthesis (45). Thus, we

433   hypothesize DacB1 and MAB_0519 are involved in septal PG synthesis and may work with

434   PBP-lipo to ensure proper septum formation. Interestingly, DacB1 and MAB_0519 are not

435   functionally redundant, given that both genes are synergistic with PBP-lipo. Further

436   characterization of the PG enzymes in *Mab* and their genetic networks will uncover species-

437   specific nuances in *Mab* PG synthesis that have the potential to be exploited for drug discovery.

438

439   Knockdown of PBP-lipo dramatically sensitized the reference *Mab* strain and 11 clinical isolates

440   to several antibiotics. The PBP-lipo knockdown was greater than 128-fold more sensitive to β-

441   lactams, ampicillin and amoxicillin, while other β-lactams like meropenem, cephalexin, ticarcillin

442   and others showed no difference in MIC. This result indicates a specific chemical-genetic

443   interaction between ampicillin/amoxicillin, and PBP-lipo. Historically, β-lactams have not been

444   used to treat *Mab* infections due to high levels of resistance and the presence of β-lactamases

445   (20). While imipenem and cefoxitin are used with some success, macrolides and

446   aminoglycosides remain the backbone of *Mab* treatment (46). Recently, studies have shown

447   dual β-lactam strategies are effective in killing *Mab* both *in vitro* and *in vivo* (47–49). These

448   synergy data suggest that understanding the specific antibiotic targets of β-lactams in *Mab*

449   would augment the design of effective dual β-lactam combinations. At the moment, effective

450   combinations are tested empirically with no insight into potential mechanisms (48). To address

451   this, Sayed *et al* used a combination of a bocillin FL binding assay to stain all the PBPs in *Mab*

452   followed by proteomics to identify the targets of 12 β-lactams and 2 β-lactamases. Interestingly,

453   in their datasets, PBP-lipo was not identified by mass spectrometry of bocillin FL-bounded PBPs

454   (50). This further supports our observation that PBP-lipo is expressed at low-levels in *Mab* and

455   is not identifiable by bocillin FL under native expression conditions.

456

457   Nonetheless, our data demonstrate that using a β-lactam or small molecules that target PBP-

458   lipo would not only kill the cell, but also potentiate β-lactams like ampicillin and amoxicillin. In

459   addition, the permeabilizing effect of PBP-lipo inhibition would potentiate drugs by allowing more

460   to enter the cell. Crucially, the observed synergy with PBP-lipo knockdown and β-lactams was

461   not just limited to the reference strain, but also present in 11 clinical isolates of *Mab,* indicating

462   that this synergy can be targeted for use in *Mab* clinical isolates.

463

464   Overall, this work employed TnSeq to identify the uniquely essential gene PBP-lipo in *Mab*. We

465   present PBP-lipo as a promising drug target given both its essentiality and its role in sensitizing

466   *Mab* to a range of antibiotics, including commonly used and accessible antibiotics, ampicillin

467   and amoxicillin. Future studies exploring the PBP networks of mycobacteria can expose further

468   species-specific vulnerabilities in peptidoglycan synthesis. Finally, identifying chemical inhibitors

469   of PBP-lipo may help form the foundation for new treatments against this emerging and difficult

470   to treat pathogen.

471 **Materials and Methods**

472

473 A full list of the strains, plasmids, and primers is available in Supplemental Tables 7, 8, and 9

474 respectively.

475
476 **Bacterial Strains and Culture Conditions:** All *M. abscessus (Mab)* and *M. tuberculosis (Mtb)*

477 strains were grown shaking at 37°C in liquid 7H9 media consisting of Middlebrook 7H9 salts

478 with 0.2% glycerol, 0.85 g/L NaCl, OADC (oleic acid, 5 g/L albumin, 2 g/L dextrose, 0.003 g/L

479 catalase), and 0.05% Tween80. *Mab* and *Mtb* were plated on Middlebrook 7H10 agar

480 supplemented with 0.5% glycerol. *M. smegmatis* mc2 155 *(Msm)* was grown shaking at 37°C in

481 liquid on 7H9 media consisting of Middlebrook 7H9 salts with 0.2% glycerol, 0.85 g/L NaCl,

482 ADC, and 0.05% Tween80 and plated on LB agar. Antibiotic selection concentrations for *Mab*

483 cultures were kanamycin 50 µg/µl and zeocin 100 µg/µl. For transposon mutant selection, 100

484 µg/ml of kanamycin was used. Antibiotic selection concentrations for *Msm* and *Mtb* cultures

485 were kanamycin 25 µg/µl, zeocin 20 µg/µl, and gentamicin 5 µg/µl. For *E. coli* (TOP10, XL1-

486 Blue and DH5α), all antibiotic concentrations were twice those of the concentrations used for

487 *Msm* and *Mtb*. Induction of all CRISPRi plasmids was performed with 500 ng/ul anhydrous

488 tetracycline (ATc).

489

490 **Strain Construction**

491 *Construction of 0, 1, 2, 3 sgRNA PBP-lipo knockdown strains and PBP-lipo complement strains*

492 To build the 0 sgRNA (empty sgRNA) *Mab* strain, we transformed the pCT296 vector containing

493 an empty sgRNA into *Mab.* To build the 1, 2, and 3 sgRNA strains, first we built individual

494 CRISPRi plasmids containing single sgRNAs that targeted PBP-lipo. These plasmids were cr25,

495 cr26, and cr56. We then designed primers that amplified the sgRNA targeting region with the

496 appropriate flanking sequences and performed Golden Gate cloning to combine the inserts into

497 one vector. This method was previously described by Rock et al (23). For the 1 sgRNA strain,

20

498 we transformed cr25 into the *Mab* strain. For the 2 sgRNA, we transformed the vector pCRC1,

499 which contained the cr25 and cr26 sgRNAs on one backbone. Finally, for the 3 sgRNA strain we

500 transformed pCRC2, which contained the cr25, cr26, and cr56 sgRNAs on one backbone.

501 To build the PBP-lipo complement strain, we designed primers to amplify PBP-lipo with modified

502 protospacer adjacent motif (PAM) sequences that were no longer homologous to the 1, 2, and 3

503 sgRNAs. This recoded PBP-lipo was then cloned into a constitutive expression vector resulting

504 in the pCA323 construct, which was transformed into the 2 sgRNA strain. The catalytically dead

505 mutant version of the recoded PBP-lipo was generated by using primers to generate the S364A

506 mutation. This engineered PBP-lipo was cloned into a constitutive expression vector and the

507 resulting construct, pCA324 was transformed into the 2 sgRNA strain.

508

509 *Msm* and *Mtb* ΔPBP-lipo strains

510 To generate PBP-lipo knockout mutants in *Msm* and *Mtb,* we used a recombineering approach

511 to replace the endogenous copy of the gene with a zeocin resistance cassette as previously

512 described (51). First, 500 base pairs of upstream and downstream sequence surrounding PBP-

513 lipo (*Rv2864c* and *MSMEG_2584c*) were amplified by PCR KOD XtremeTM Hot Start DNA

514 polymerase (EMD Millipore, Billerica, MA). These flanking regions were amplified with overlaps

515 for the zeocin resistance cassette. The 2 flanking regions and zeocin resistance cassette were

516 then assembled via isothermal assembly (52) into a single construct, which was then amplified

517 by PCR. Each deletion construct was transformed into either *Mtb* or *Msm* expressing inducible

518 copies of RecET for recombination (53). The resulting colonies were screened for PBP-lipo

519 deletion by PCR.

520

521 *PBP-lipo_{Mab}-strep expression strain*

522 PBP-lipo$_{Mab}$ was amplified using primers that added a C-terminal strep tag to the protein. The

523 resulting insert was Gibson stitched to the vector backbone that drove expression of PBP-

524 lipo$_{Mab}$-strep from the constitutively active MOP promoter.

525

526 *mRFP-PBP-lipo$_{Mab}$*

527 We amplified PBP-lipo$_{Mab}$ in two fragments. The first fragment contained the N-terminal signal

528 sequence of PBP-lipo. The second fragment contained the remainder of the protein. We then

529 amplified mRFP with overhangs that were compatible with the two halves of PBP-lipo. The

530 resulting three fragments were Gibson assembled to a vector backbone that constitutively drove

531 expression of the mRFP-PBP-lipo$_{Mab}$ fusion protein. A gly-gly-ser-gly-ser-gly linker was used in

532 between mRFP and the new N & C terminus of PBP-lipo.

533

534 *DacB1-GFPmut3*

535 DacB1 lacking a stop codon was amplified along with GFPmut3 containing overlaps with DacB1

536 and a gly-gly-ser linker. The two fragments were Gibson assembled to a vector backbone that

537 constitutively drove expression of the DacB1-GFPmut3 fusion protein.

538

539 **Growth Curve:** *Mab, Msm,* and *Mtb* cultures were grown to log phase and diluted to OD600

540 0.05. Growth curves were performed in a 96 well format at 37°C with shaking. OD600 was

541 measured every 15 min for 24-72 hr using the TECAN plate reader

542

543 **Colony Forming Units:** *Mab* and *Msm* cultures were grown to mid-log phase and then serially

544 diluted in their respective media in 96 well plates. Dilutions were then spot plated onto solid

545 media +/- 500 ng/ul ATc. Plates were incubated at 37°C for 4 days *(Mab)* or 3 days *(Msm)*. After

546 incubation, the resulting CFUs were calculated by counting the number of colonies at the

547 appropriate dilution. The fraction survivability was calculated as CFUs +ATc / -ATc.

22

548

549   **Minimum Inhibitory Concentration Determination:** *Mab, Msm,* and *Mtb* were grown to mid-

550   log phase and diluted to an OD600 = 0.003 in each well of non-treated 96-well plates (Genesee

551   Scientific) containing 100 μL of antibiotic serially diluted in 7H9 + OADC + 5 μg/mL clavulanate

552   (Sigma Aldrich). For MICs on *Mab* knockdown cells, cultures were induced for knockdown 18 hr

553   prior with 500 ng/ul ATc. Wells with knockdown bacteria also contained 500 ng/ul ATc. *Msm*

554   media contained ADC rather than OADC. Cells were incubated with drug at 37°C with shaking

555   for 1 day *(Mab, Msm)* or 7 days *(Mtb)*. Afterwards, 0.002% resazurin diluted in ddH$_2$O (Sigma

556   Aldrich) was added to each well. Plates were then incubated for 24 hr. MICs were determined

557   by the concentration of antibiotic that turned wells blue signifying no metabolic activity (54).

558

559   **Generation of Transposon Libraries:** To create transposon mutant libraries of *Mab* ATCC

560   19977 and *Msm* (wildtype and ΔPBP-lipo), 100 ml of bacterial cultures were grown to an OD600

561   of 1.5 – 2.0. For *Mab*, cultures were grown in biological triplicate. For *Msm*, the wildtype strain

562   was grown in duplicate while one replicate of the ΔPBP-lipo strain was grown. The cells were

563   then washed twice with 50 ml of MP Buffer (50mM Tris-HCl pH 7.5, 150 mM NaCl, 10 mM

564   MgSO$_4$, 2 mM CaCl$_2$) and resuspended in 1/10th the culture volume in MP Buffer. Afterwards, 2

565   x 10^{11} pfu of temperature sensitive φMycoMarT7 phage carrying the Himar1 transposon were

566   added to bacteria. Phage and bacterial cultures were incubated at 37°C for 4 hr with shaking.

567   The transduced cultures were spun down at RT 4000 rpm for 10 min and resuspended in 12 ml

568   of PBS-Tween. The cultures were then tittered by plating on 7H10 plates *(Mab)* or LB *(Msm)*

569   supplemented with kanamycin 100 μg/μml *(Mab)* or 20 μg/μl *(Msm)* before freezing the aliquots

570   for future plating. After determining the titer, 150,000 bacterial mutants of each transduced

571   culture were plated onto kanamycin selective plates and grown for 4 days at 37°C. The resulting

572   mutant libraries were harvested and stored in aliquots with 7H9 + 10% glycerol at -80°C.

573

574 **Genomic DNA Extraction:** To prep libraries for sequencing, we isolated the gDNA of the

575 mutant libraries using a bead-beating protocol developed in the lab. 2-6 ml of transposon mutant

576 libraries were thawed and spun down to remove excess glycerol in the sample. Pellets were

577 then resuspended in TE Buffer (10 mM Tris HCl pH 7.4, 1 mM EDTA pH8) and placed in bead-

578 beating tubes with 600 µl of phenol:chloroform. The samples were then bead-beat 4X for 45 s at

579 4000 rpm. Samples were cooled on ice for 45 s between each successive bead-beat round.

580 After bead-beating, the samples were spun down for 10 min at 13,000 rpm. The supernatant

581 was transferred to a new falcon tube and incubated with 1:1 volume phenol-chloroform for 1 hr

582 rocking. Samples were then spun down in MaXtract High Density phase-lock tubes (Qiagen) at

583 1500 g for 5 min. This separated the aqueous and organic layers. Afterwards, ½ volume of

584 chloroform was added to the tube and the contents were spun down at 1500 g for 5 min. The

585 aqueous phase was transferred to a new tube and RNAse A (Thermo Fisher) was added to a

586 final concentration of 25 µg/µl. The tubes were incubated at 37°C for 1 hr with shaking. Finally,

587 the supernatant was washed with 1:1 volume of phenol-chloroform followed by ½ volume of

588 chloroform. The aqueous phase was transferred to a new tube and genomic DNA was

589 precipitated with 1 volume of isopropanol alcohol and 1/10th volume of 3 M sodium acetate pH

590 5.2. The library gDNA was washed twice with fresh 70% ethanol and resuspended in nuclease

591 free ddH$_2$O. This protocol consistently generated high yields of *Mab* gDNA.

592

593 **Transposon sequencing, mapping, and analysis:** Sequencing libraries were prepared from

594 the extracted gDNA by amplifying chromosomal-transposon junctions following the protocol as

595 described by Long et al, 2015 (21). These amplicons were then sequenced using the Illumina

596 Hi-Seq platform. The resulting reads were mapped onto the *Mab* or *Msm* genomes. The data

597 were analyzed using the TRANSIT pipeline (22). Insertion counts at each TA site were

598 normalized using TTR normalization and averaged across replicates. Essentiality categories of

599 genes were determined by the Hidden Markov Model (HMM) algorithm in TRANSIT.

600   Resampling analysis was used to compare insertion accounts between genes in the wildtype

601   and ΔPBP-lipo *Msm* strains.

602

603   **Cloning of CRISPRi Constructs:** To clone sgRNAs onto the CRISPRi vector backbone,

604   complimentary targeting oligos were annealed and ligated (T4 DNA ligase, NEB) into the BsmBI

605   digested CRISPRi vector backbone. To clone multiple sgRNAs into the same vector, the

606   promoter, sgRNA handle, and sgRNA sequences were amplified with the appropriate flanking

607   sequences to perform Golden Gate cloning using the SapI cloning site in the CRISPRi vector

608   (23). All cloning was performed using DH5a cells and sequences were verified before

609   transformation into *Mab* and *Msm.*

610

611   **Transformation of *M. abscessus*:** To generate electrocompetent *Mab* cells, 50 ml of *Mab*

612   cultures were grown to mid-log phase. Cells were spun down at 4000 rpm for 10 min and

613   washed twice with pre-chilled 10% glycerol. Cell pellets were resuspended in 1/100th of the

614   starting volume and kept on ice for immediate use or stored at -80°C for future use. For

615   transformations ~100 ng of plasmid DNA was incubated with electro-competent cells for 5 min

616   before transforming the cells with 2500 V, 125 Ω, 25 μF. Afterwards, cells were recovered in 1

617   ml of 7H10 with OADC without selection for 3 hr at 37°C with shaking. Cells were then plated on

618   7H10 with the appropriate selection marker and incubated for 4 days at 37°C.

619

620   **Microscopy and Image Analysis:** All imaging was performed on an inverted Nikon TI-E

621   microscope at 60X and 100X magnification. For PBP-lipo knockdown experiments, cultures

622   were induced for knockdown with 500 ng/ul ATc for 18 hr prior to imaging. All *Mab* cultures were

623   fixed with 7H9 + 3% paraformaldehyde (PFA) for 1 hr and resuspended in PBS + 0.05%

624   Tween80 prior to imaging. Cellular features including cell length, width, and fluorescence signal

625   were analyzed using the OMEGA image analysis pipeline developed in the lab (Zhu et al,

626   unpublished).

627

628   **Fluorescent D-Amino Acid Staining:** NADA (3-[(7-Nitro-2,1,3-benzoxadiazol-4-yl)amino]-D-

629   alanine hydrochloride) was synthesized by Tocris following the published protocol (27). To stain

630   *Mab* with NADA, 0.1 mM of FDAA was added to 1 ml of exponentially growing cells and

631   incubated for 3 min before washing in warm 7H9 twice. For *Mab* imaging, after the second

632   wash, cells were fixed in 7H9 + 3% paraformaldehyde for 1 hr. The PFA was then washed off

633   and cells were resuspended in PBS + 0.05% Tween80 prior to imaging.

634

635   **RNA Extraction and RT-qPCR:** For each strain, cultures were grown in biological triplicate to

636   mid-log phase and then diluted back in +/- 500 ng/ml ATc and grown for 18 hr to achieve target

637   knockdown. Afterwards, 2 OD600 equivalents of cells from each culture were harvested by

638   centrifugation, resuspended in TRIzol (Thermo Fisher), and lysed by bead beating (Lysing

639   Matrix B, MP Biomedicals). Total RNA was extracted using the RNA miniprep (Zymo Research).

640   Residual genomic DNA was digested with TURBO DNase (Ambion), and samples were cleaned

641   with RNA clean-up columns (Zymo Research). cDNA was prepared using random hexamers

642   following manual instructions (Life Technologies Superscript IV). Alkaline hydrolysis was then

643   used to remove RNA. cDNA was purified by spin column (Qiagen) and then quantified by real-

644   time quantitative PCR (RT–qPCR) on a Viia7 light cycler (Applied Biosystems) using iTaq

645   Universal SYBR Green Supermix (BioRad). All qPCR primer pairs were confirmed to be >95%

646   efficient. The masses of cDNA used were experimentally validated to be within the linear

647   dynamic range of the assay. Signals were normalized to the *sigA* (*MAB_3009*) transcript and

648   quantified by the ΔΔCt method. Error bars are standard deviations from three biological

649   replicates.

650

651   **Bocillin FL staining:** *Mab* cultures were grown to mid-log phase and 10 OD units of bacteria

652   were spun down and resuspended in 1ml of fresh 7H9 media with 5 µg/ml of clavulanate.

653   Bocillin-BODIPY or FITC were added to cultures to a final concentration of 10 µM. Cells were

654   then incubated at 37°C for 2.5 hr, with aluminum wrapping to prevent light exposure. After

655   labeling, cells are washed with PBS + 0.05% Tween80 three times and resuspended in 200 µl

656   of lysis buffer (50 mM Tris-HCl pH = 7.4, 50 mM NaCl, protease inhibitor (Roche)). Samples

657   were bead beat 4X at 4000 rpm for 1 min with 1 min of rest on ice in between rounds of bead-

658   beats. $CaCl_2$ was added to a final concentration of 1 mM along with 4U of DNAse I and 10

659   mg/ml of fresh lysozyme. Samples were incubated at 37°C for 30 min. Afterwards, supernatants

660   were normalized by A280 protein concentration, diluted with 6X Laemmli buffer, and run on 4%–

661   12% NuPAGE Bis Tris precast gels (Life Technologies). To visualize fluorescence, we used a

662   BioRad Gel Doc system. To detect the presence of PBP-lipo-strep, we performed a Western

663   Blot. Membranes were blotted with rabbit α-Strep (GenScript) at 1:1000 in TBST + 3% BSA.

664

665   **Calcein Staining:** For each strain, cultures were grown in biological triplicate to mid-log phase

666   and diluted back in +/- 500 ng/ml ATc and grown for 18 hr to achieve target knockdown.

667   Afterwards, 3 OD units of bacteria were washed twice with PBS + 0.05% Tween80. Cells were

668   resuspended in PBS + 0.05% Tween80 and 100 µl of cells at OD600 = 0.4 was added to 96

669   well plates. The plates were incubated in the plate reader for 30 min at 37°C with shaking.

670   Afterwards, calcein was added at a final concentration of 1 µg/ml. Fluorescence signal was

671   measured every minute using the Tecan plate reader.

672

27

673 **Acknowledgements**
674
680
681

References

1. Bryant JM, Grogono DM, Rodriguez-Rincon D, Everall I, Brown KP, Moreno P, et al. Emergence and spread of a human-transmissible multidrug-resistant nontuberculous mycobacterium. Science. 2016 Nov 11;354(6313):751–7.

2. Primm TP, Lucero CA, Falkinham JO. Health impacts of environmental mycobacteria. Clin Microbiol Rev. 2004 Jan;17(1):98–106.

3. Johansen MD, Herrmann J-L, Kremer L. Non-tuberculous mycobacteria and the rise of Mycobacterium abscessus. Nat Rev Microbiol. 2020 Feb 21;1–16.

4. Nessar R, Cambau E, Reyrat JM, Murray A, Gicquel B. Mycobacterium abscessus: a new antibiotic nightmare. J Antimicrob Chemother. 2012 Apr;67(4):810–8.

5. Pang H, Li G, Wan L, Jiang Y, Liu H, Zhao X, et al. In vitro drug susceptibility of 40 international reference rapidly growing mycobacteria to 20 antimicrobial agents. Int J Clin Exp Med. 2015;8(9):15423–31.

6. Jarand J, Levin A, Zhang L, Huitt G, Mitchell JD, Daley CL. Clinical and microbiologic outcomes in patients receiving treatment for Mycobacterium abscessus pulmonary disease. Clin Infect Dis Off Publ Infect Dis Soc Am. 2011 Mar 1;52(5):565–71.

7. Bryant JM, Brown KP, Burbaud S, Everall I, Belardinelli JM, Rodriguez-Rincon D, et al. Stepwise pathogenic evolution of Mycobacterium abscessus. Science [Internet]. 2021 Apr 30 [cited 2021 Jun 18];372(6541).

8. van Opijnen T, Camilli A. Transposon insertion sequencing: a new tool for systems-level analysis of microorganisms. Nat Rev Microbiol. 2013 Jul;11(7):435–42.

9. DeJesus MA, Gerrick ER, Xu W, Park SW, Long JE, Boutte CC, et al. Comprehensive Essentiality Analysis of the Mycobacterium tuberculosis Genome via Saturating Transposon Mutagenesis. mBio [Internet]. 2017 Mar 8 [cited 2020 Mar 28];8(1).

10. Foreman M, Gershoni M, Barkan D. A Simplified and Efficient Method for Himar-1 Transposon Sequencing in Bacteria, Demonstrated by Creation and Analysis of a Saturated Transposon-Mutant Library in Mycobacterium abscessus. mSystems [Internet]. 2020 Oct 27 [cited 2021 Mar 7];5(5).

11. Laencina L, Dubois V, Le Moigne V, Viljoen A, Majlessi L, Pritchard J, et al. Identification of genes required for Mycobacterium abscessus growth in vivo with a prominent role of the ESX-4 locus. Proc Natl Acad Sci U S A. 2018 30;115(5):E1002–11.

12. Rifat D, Chen L, Kreiswirth BN, Nuermberger EL. Genome-Wide Essentiality Analysis of Mycobacterium abscessus by Saturated Transposon Mutagenesis and Deep Sequencing. mBio. 2021 Jun 15;e0104921.

13. Wong EB, Cohen KA, Bishai WR. Rising to the challenge: New therapies for tuberculosis. Vol. 21, Trends in Microbiology. 2013. p. 493–501.

14. Bhat ZS, Rather MA, Maqbool M, Lah HU, Yousuf SK, Ahmad Z. Cell wall: A versatile fountain of drug targets   in Mycobacterium tuberculosis. Vol. 95, Biomedicine and Pharmacotherapy. 2017. p. 1520–34.

15. Jarlier V, Nikaido H. Mycobacterial cell wall: Structure and role in natural resistance to antibiotics. FEMS Microbiol Lett. 1994 Oct 1;123(1–2):11–8.

16. Nasiri MJ, Haeili M, Ghazi M, Goudarzi H, Pormohammad A, Imani Fooladi AA, et al. New Insights in to the Intrinsic and Acquired Drug Resistance Mechanisms in Mycobacteria. Front Microbiol. 2017 Apr 25;8:681.

17. Kieser KJ, Rubin EJ. How sisters grow apart: Mycobacterial growth and division. Vol. 12, Nature Reviews Microbiology. Nature Publishing Group; 2014. p. 550–62.

18. Arora D, Chawla Y, Malakar B, Singh A, Nandicoori VK. The transpeptidase PbpA and noncanonical transglycosylase RodA of Mycobacterium tuberculosis play important roles in regulating bacterial cell lengths. J Biol Chem. 2018 Apr 27;293(17):6497–516.

19. Slayden RA, Belisle JT. Morphological features and signature gene response elicited by inactivation of FtsI in Mycobacterium tuberculosis. J Antimicrob Chemother. 2009 Mar 1;63(3):451–7.

20. Soroka D, Dubée V, Soulier-Escrihuela O, Cuinet G, Hugonnet J-E, Gutmann L, et al. Characterization of broad-spectrum Mycobacterium abscessus class A β-lactamase. J Antimicrob Chemother. 2014 Mar;69(3):691–6.

21. Long JE, DeJesus M, Ward D, Baker RE, Ioerger T, Sassetti CM. Identifying essential genes in Mycobacterium tuberculosis by global phenotypic profiling. Methods Mol Biol Clifton NJ. 2015;1279:79–95.

22. DeJesus MA, Ambadipudi C, Baker R, Sassetti C, Ioerger TR. TRANSIT--A Software Tool for Himar1 TnSeq Analysis. PLoS Comput Biol. 2015 Oct;11(10):e1004401.

23. Rock JM, Hopkins FF, Chavez A, Diallo M, Chase MR, Gerrick ER, et al. Programmable transcriptional repression in mycobacteria using an orthogonal CRISPR interference platform. Nat Microbiol. 2017 Feb 6;2(4):1–9.

24. Peters JM, Koo B-M, Patino R, Heussler GE, Hearne CC, Qu J, et al. Enabling genetic analysis of diverse bacteria with Mobile-CRISPRi. Nat Microbiol. 2019 Feb;4(2):244–50.

25. Caro F, Place NM, Mekalanos JJ. Analysis of lipoprotein transport depletion in Vibrio cholerae using CRISPRi. Proc Natl Acad Sci. 2019 Aug 20;116(34):17013–22.

26. Zhao G, Meier TI, Kahl SD, Gee KR, Blaszczak LC. BOCILLIN FL, a sensitive and commercially available reagent for detection of penicillin-binding proteins. Antimicrob Agents Chemother. 1999 May;43(5):1124–8.

27. Kuru E, Tekkam S, Hall E, Brun YV, Van Nieuwenhze MS. Synthesis of fluorescent D-amino acids and their use for probing peptidoglycan synthesis and bacterial growth in situ. Nat Protoc. 2015 Jan;10(1):33–52.

28. Wu KJ, Zhang J, Baranowski C, Leung V, Rego EH, Morita YS, et al. Characterization of Conserved and Novel Septal Factors in Mycobacterium smegmatis. J Bacteriol. 2018 15;200(6).

29. Baranowski C, Welsh MA, Sham L-T, Eskandarian HA, Lim HC, Kieser KJ, et al. Maturing Mycobacterium smegmatis peptidoglycan requires non-canonical crosslinks to maintain shape. eLife. 2018 16;7.

30. Kieser KJ, Baranowski C, Chao MC, Long JE, Sassetti CM, Waldor MK, et al. Peptidoglycan synthesis in Mycobacterium tuberculosis is organized into networks with varying drug susceptibility. Proc Natl Acad Sci U S A. 2015 Oct 20;112(42):13087–92.

761   31. Slayden RA, Belisle JT. Morphological features and signature gene response elicited by inactivation
762   of FtsI in Mycobacterium tuberculosis. J Antimicrob Chemother. 2009 Mar;63(3):451–7.

763   32. Wissel MC, Weiss DS. Genetic Analysis of the Cell Division Protein FtsI (PBP3): Amino Acid
764   Substitutions That Impair Septal Localization of FtsI and Recruitment of FtsN. J Bacteriol. 2004
765   Jan;186(2):490–502.

766   33. Datta P, Dasgupta A, Singh AK, Mukherjee P, Kundu M, Basu J. Interaction between FtsW and
767   penicillin-binding protein 3 (PBP3) directs PBP3 to mid-cell, controls cell septation and mediates the
768   formation of a trimeric complex involving FtsZ, FtsW and PBP3 in mycobacteria. Mol Microbiol.
769   2006 Dec;62(6):1655–73.

770   34. Tortoli E, Kohl TA, Brown-Elliott BA, Trovato A, Leão SC, Garcia MJ, et al. Emended description of
771   Mycobacterium abscessus, Mycobacterium abscessus subsp. abscessus and
772   Mycobacteriumabscessus subsp. bolletii and designation of Mycobacteriumabscessus subsp.
773   massiliense comb. nov. Int J Syst Evol Microbiol. 2016 Nov;66(11):4471–9.

774   35. Allison F. Carey, Rock JM, Krieger IV, Chase MR, Fernandez-Suarez M, Gagneux S, et al. TnSeq of
775   Mycobacterium tuberculosis clinical isolates reveals strain-specific antibiotic liabilities. PLOS
776   Pathog. 2018 Mar 5;14(3):e1006939.

777   36. Medjahed H, Reyrat J-M. Construction of Mycobacterium abscessus defined glycopeptidolipid
778   mutants: comparison of genetic tools. Appl Environ Microbiol. 2009 Mar;75(5):1331–8.

779   37. Kieser KJ, Rubin EJ. How sisters grow apart: mycobacterial growth and division. Nat Rev Microbiol.
780   2014 Aug;12(8):550–62.

781   38. Datta P, Dasgupta A, Singh AK, Mukherjee P, Kundu M, Basu J. Interaction between FtsW and
782   penicillin-binding protein 3 (PBP3) directs PBP3 to mid-cell, controls cell septation and mediates the
783   formation of a trimeric complex involving FtsZ, FtsW and PBP3 in mycobacteria. Mol Microbiol.
784   2006 Dec;62(6):1655–73.

785   39. Rajagopalan M, Maloney E, Dziadek J, Poplawska M, Lofton H, Chauhan A, et al. Genetic evidence
786   that mycobacterial FtsZ and FtsW proteins interact, and colocalize to the division site in
787   Mycobacterium smegmatis. FEMS Microbiol Lett. 2005 Sep 1;250(1):9–17.

788   40. Datta P, Dasgupta A, Bhakta S, Basu J. Interaction between FtsZ and FtsW of Mycobacterium
789   tuberculosis *. J Biol Chem. 2002 Jul 12;277(28):24983–7.

790   41. Botella H, Yang G, Ouerfelli O, Ehrt S, Nathan CF, Vaubourgeix J. Distinct Spatiotemporal Dynamics
791   of Peptidoglycan Synthesis between Mycobacterium smegmatis and Mycobacterium tuberculosis.
792   mBio. 2017 12;8(5).

793   42. Ghosh AS, Chowdhury C, Nelson DE. Physiological functions of D-alanine carboxypeptidases in
794   Escherichia coli. Trends Microbiol. 2008 Jul 1;16(7):309–17.

795   43. Ealand CS, Asmal R, Mashigo L, Campbell L, Kana BD. Characterization of putative DD-
796   carboxypeptidase-encoding genes in Mycobacterium smegmatis. Sci Rep. 2019 Mar 26;9(1):5194.

797   44. Gorla P, Plocinska R, Sarva K, Satsangi AT, Pandeeti E, Donnelly R, et al. MtrA Response Regulator
798   Controls Cell Division and Cell Wall Metabolism and Affects Susceptibility of Mycobacteria to the
799   First Line Antituberculosis Drugs. Front Microbiol [Internet]. 2018 Nov 23 [cited 2020 May 27];9.

800 45. Zhang W, Li S, Ma L, Ding W, Xu Y. Identification of a novel carboxypeptidase encoded by Rv3627c
801   that plays a potential role in mycobacteria morphology and cell division. Enzyme Microb Technol.
802   2019 Jul 1;126:32–40.

803 46. Novosad SA, Beekmann SE, Polgreen PM, Mackey K, Winthrop KL. Treatment of Mycobacterium
804   abscessus Infection. Emerg Infect Dis. 2016 Mar;22(3):511–4.

805 47. Story-Roller E, Maggioncalda EC, Lamichhane G. Synergistic Efficacy of β-Lactam Combinations
806   against Mycobacterium abscessus Pulmonary Infection in Mice. Antimicrob Agents Chemother.
807   2019;63(8).

808 48. Pandey R, Chen L, Manca C, Jenkins S, Glaser L, Vinnard C, et al. Dual β-Lactam Combinations
809   Highly Active against Mycobacterium abscessus Complex In Vitro. mBio [Internet]. 2019 Feb 26
810   [cited 2020 May 9];10(1).

811 49. Lopeman RC, Harrison J, Rathbone DL, Desai M, Lambert PA, Cox JAG. Effect of Amoxicillin in
812   combination with Imipenem-Relebactam against Mycobacterium abscessus. Sci Rep. 2020 Jan
813   27;10(1):928.

814 50. Sayed ARM, Shah NR, Basso KB, Kamat M, Jiao Y, Moya B, et al. First Penicillin-Binding Protein
815   Occupancy Patterns for 15 β-Lactams and β-Lactamase Inhibitors in Mycobacterium abscessus.
816   Antimicrob Agents Chemother [Internet]. 2020 Dec 16 [cited 2021 Mar 24];65(1).

817 51. Boutte CC, Baer CE, Papavinasasundaram K, Liu W, Chase MR, Meniche X, et al. A cytoplasmic
818   peptidoglycan amidase homologue controls mycobacterial cell wall synthesis. Laub M, editor. eLife.
819   2016 Jun 15;5:e14590.

820 52. Gibson DG, Young L, Chuang R-Y, Venter JC, Hutchison CA, Smith HO. Enzymatic assembly of
821   DNA molecules up to several hundred kilobases. Nat Methods. 2009 May;6(5):343–5.

822 53. Murphy KC, Papavinasasundaram K, Sassetti CM. Mycobacterial recombineering. Methods Mol Biol
823   Clifton NJ. 2015;1285:177–99.

824 54. Kieser KJ, Boutte CC, Kester JC, Baer CE, Barczak AK, Meniche X, et al. Phosphorylation of the
825   Peptidoglycan Synthase PonA1 Governs the Rate of Polar Elongation in Mycobacteria. PLOS
826   Pathog. 2015 Jun 26;11(6):e1005010.

827
828

829

Figures and Legends

Figure 1. **Overview of TnSeq Analysis. (A)** Schematic of TnSeq protocol. Phage carrying Himar1 transposon is used to transduce *Mab* ATCC 19977 cultures. Over 51,000 independent transposon mutants were generated across three libraries **(B)** Location of transposon insertions in *M. abscessus subsp. abscessus* ATCC 19977 genome. Transposon insertions represent an average of the three replicates. Black bars represent number of insertions at each TA site. **(C)** Breakdown of gene essentiality categories. Essentiality calls were determined using the Hidden Markov Model (HMM) in TRANSIT **(D)** Essentiality comparison of mutual orthologs between *Mab* and *Mtb*. Venn Diagram shows 282 mutual orthologs are essential in both species. 20 essential *Mab* genes have mutual orthologs in *Mtb* that are non-essential. **(E)** COG (Clusters of Orthologous Group) categories of essential genes in *Mab*.
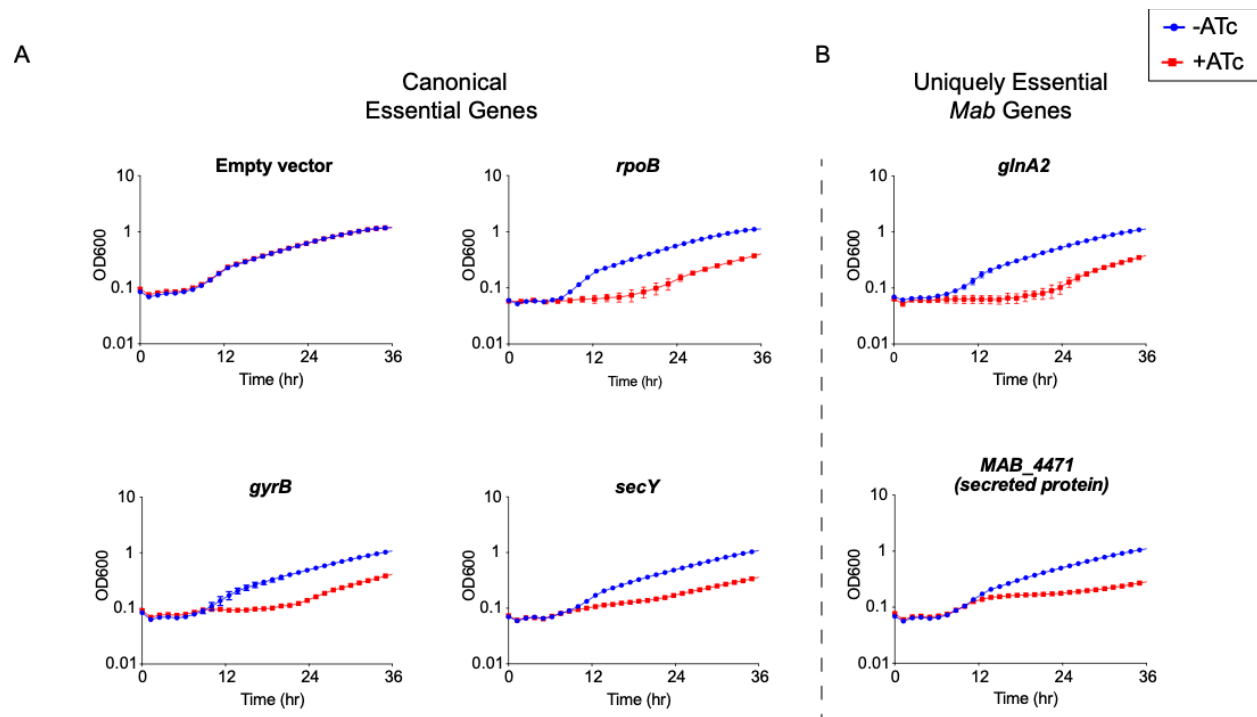
Figure 2. Validation of Essential Genes. (A) Growth curve of *Mab* strains with sgRNAs targeting canonical essential genes. **(B)** Growth curve of *Mab* strains with sgRNAs targeting uniquely essential *Mab* genes.
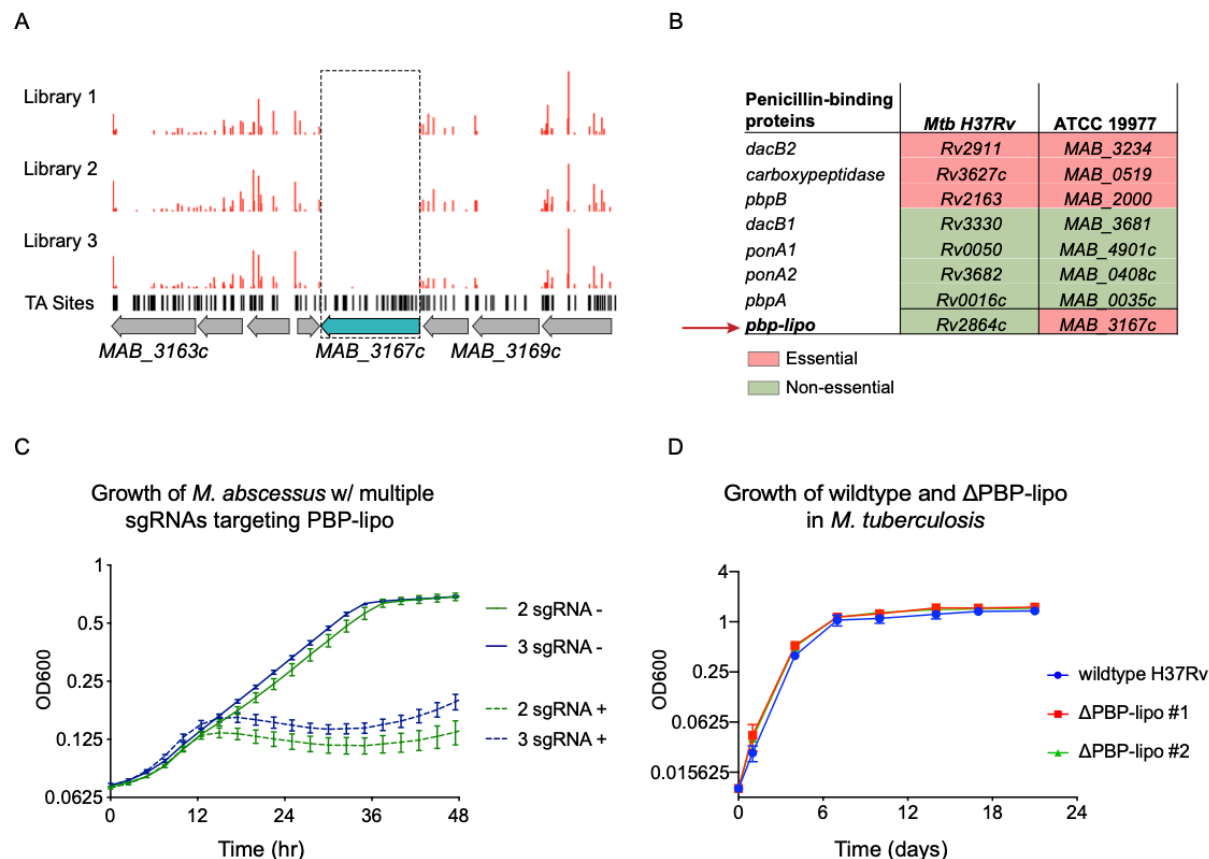
Figure 3. PBP-lipo is uniquely essential in *Mab* and non-essential in *Mtb*. (A) Transposon-insertion profile of PBP-lipo across three replicate transposon libraries. Red bars indicate the number of transposon insertions. Horizontal black lines indicate 'TA' sites, where the transposon inserts. Genes are schematized with gray arrows, with PBP-lipo colored in blue. Dotted box demarcates lack of insertions in PBP-lipo. **(B)** Comparison of essentiality for PBP orthologs between *Mtb* and *Msm*. **(C)** Growth of *Mab* cultures transformed with CRISPRi plasmid carrying either 2 or 3 sgRNAs targeting PBP-lipo. "-" symbol indicates cultures were grown without ATc. "+" symbol indicates cultures were grown with ATc. **(D)** Growth of wildtype *Mtb* and PBP-lipo knockout strains.
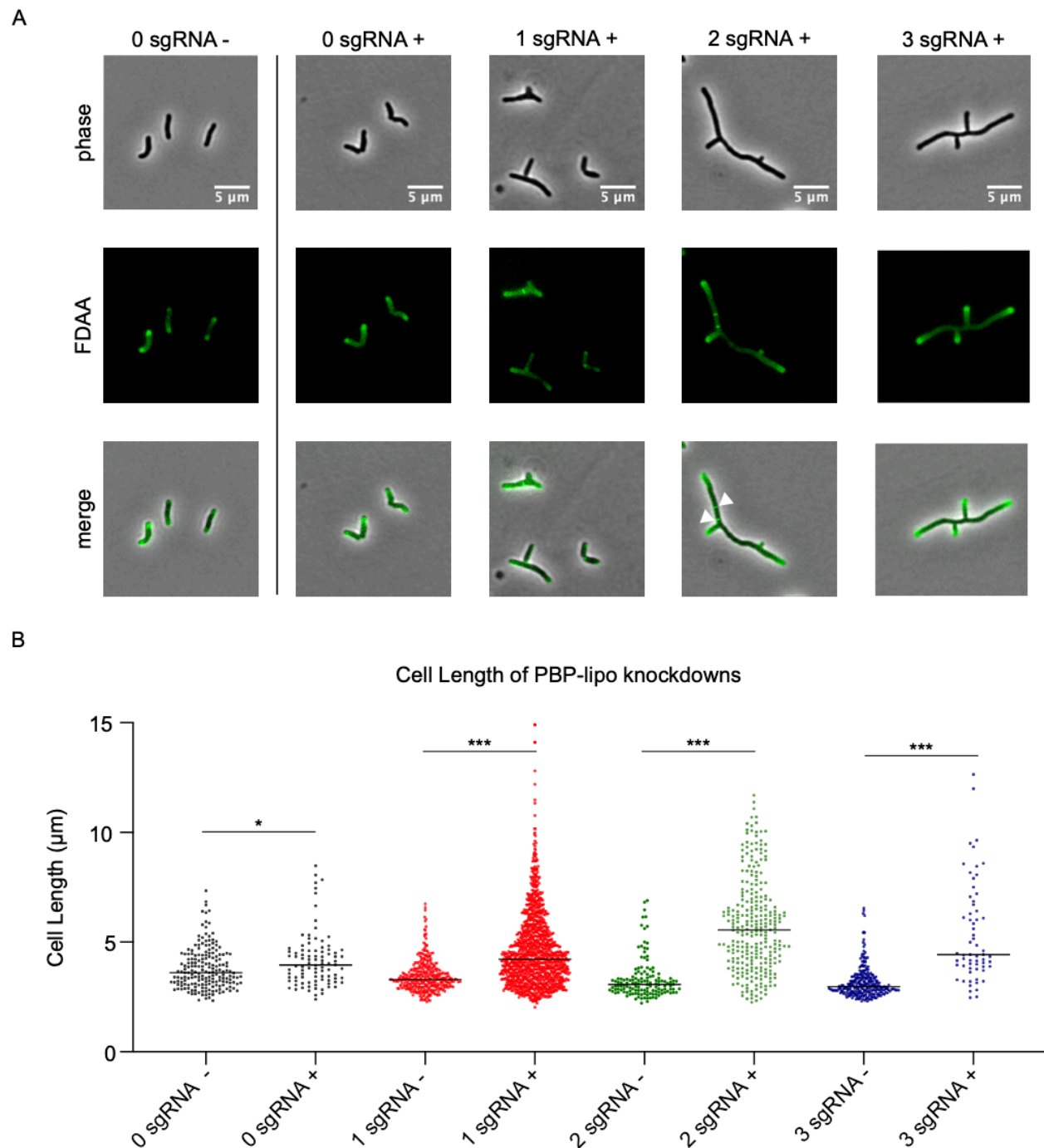
Figure 4. Knockdown of PBP-lipo disrupts cell morphology. **(A)** Microscopy images of PBP-lipo knockdown cultures. *Mab* strains carrying CRISPRi plasmids with either 0, 1, 2, or 3 sgRNAs targeting PBP-lipo. Arrows indicate sites of multiple septa formation. **(B)** Cell lengths of uninduced and induced strains. Measurements were obtained by image pipeline, OMEGA (Zhu *et al*, unpublished). Student's t test used to calculate the statistical difference in mean cell lengths. *** = p-val < 0.0001. * = p-val < 0.05.
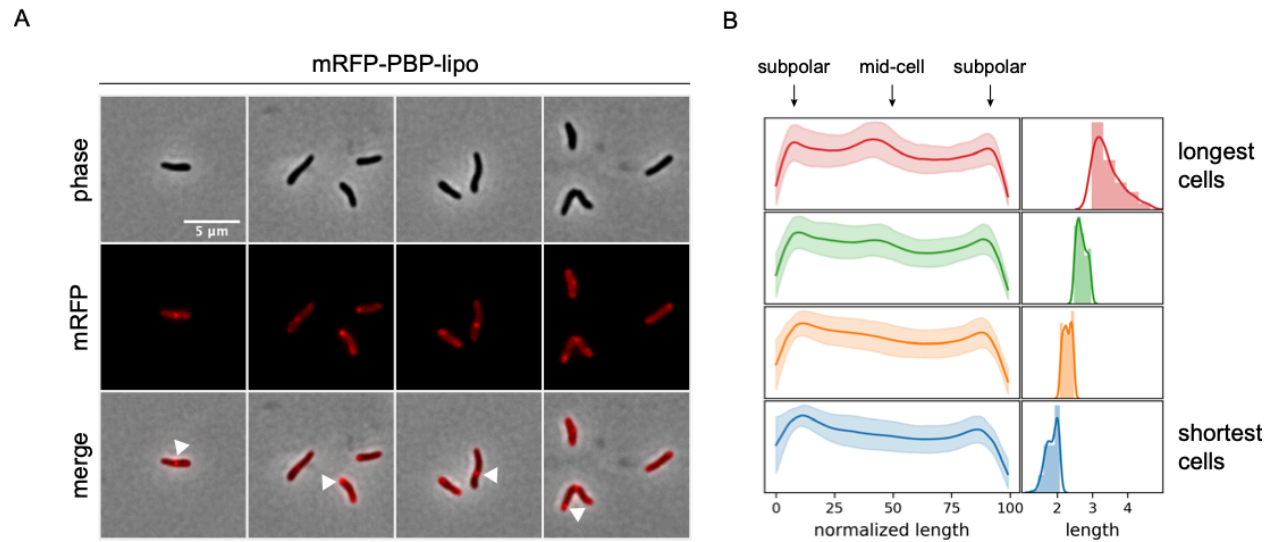
907
908
909 **Figure 5. PBP-lipo localizes to the subpolar region and the septum**. **(A)** Microscopy images of PBP-
910 lipo N-terminally tagged with mRFP. White arrows demarcate subpolar and septal localization of PBP-
911 lipo. **(B)** Quantification of mRFP signal along the length of the cell using OMEGA imaging pipeline (Zhu *et*
912 *al*, unpublished). Signal was normalized by cell length and cells were binned into quartiles based on
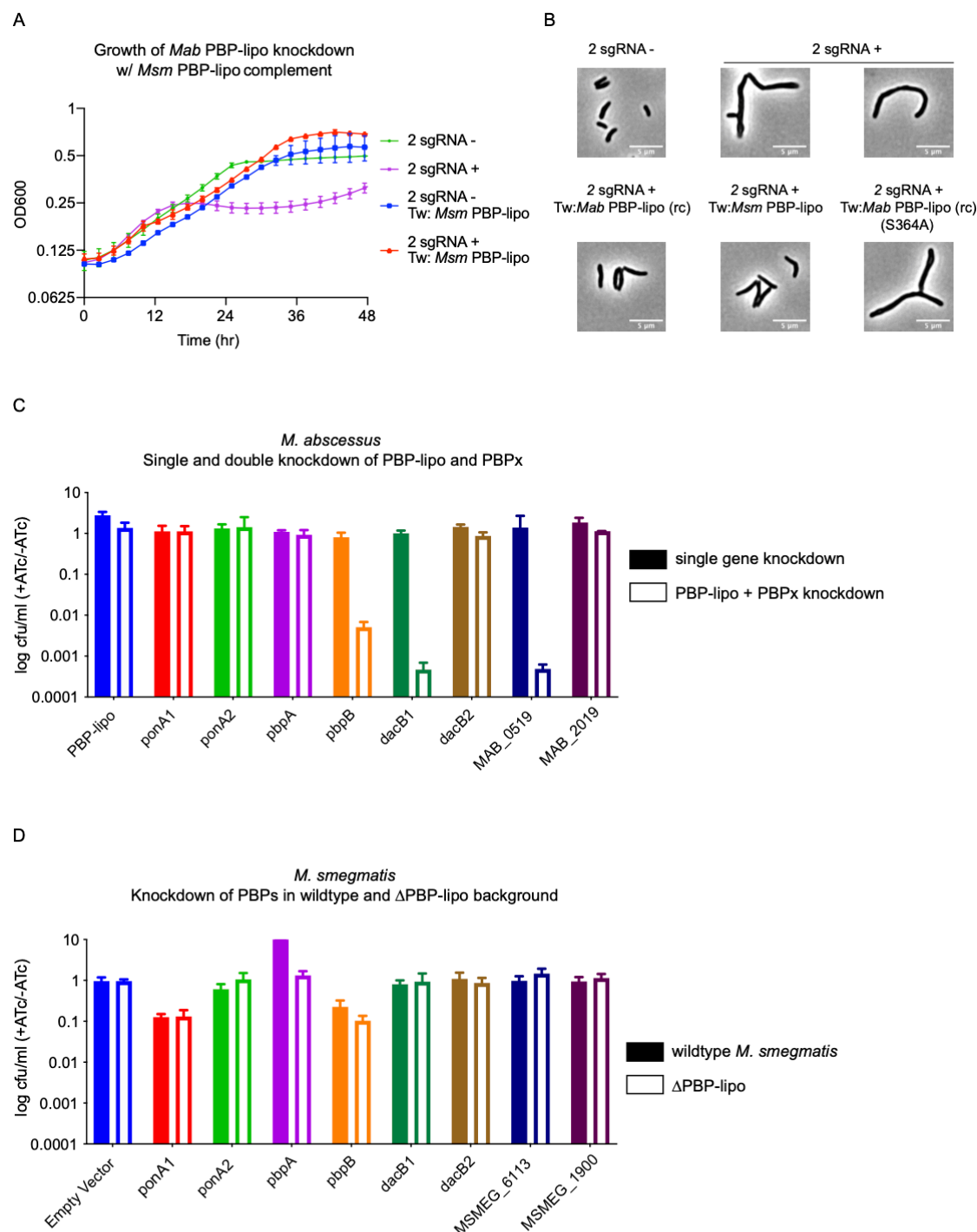913 length.
914

915
916
Figure 6. PBP-lipo network in *Mab* does not exist in *Msm*. (A) Growth curve of 2 sgRNA strain
targeting PBP-lipo and 2 sgRNA strain with a constitutively expressed copy of PBP-lipo$_{Msm}$. **(B)**
Microscopy images of 2 sgRNA and PBP-lipo complement strains. **(C)** Genetic synergy of PBP-lipo with
other PBPs in *Mab*. Solid bar represents CFU of strains where a single PBP was knocked down. Open
bar represents strains where PBP-lipo was knocked down in combination with the listed PBP. **(D)** Genetic
synergy of PBPs and PBP-lipo in *Msm.* CRISPRi plasmids carrying sgRNAs targeting each of the PBPs in
Msm were transformed into wildtype *Msm* (closed bar) and the ΔPBP-lipo mutant (open bar).
924

Table 1: Minimum Inhibitory Concentration (MIC) (µg/ml)
of ATCC 19977 +/- PBP-lipo Knockdown

Antibiotic	-ATc	+ATc	Fold Difference
Cell Wall			
Ampicillin	>256	2	>128X
Amoxicillin	>256	2	>128X
Faropenem	8	1	8X
Cefoxitin	8	2	4X
Vancomycin	8	2	4X
Meropenem	128	128	N/A
Imipenem	>64	>64	" "
Ticarcillin	>64	>64	" "
Ceftazidime	>64	>64	" "
Cephalexin	>64	>64	" "
Ceftazidime	>64	>64	" "
D-Cycloserine	>64	>64	" "
Ethambutol	>64	>64	" "
Isoniazid	>512	>512	" "
Ribosome			
Clarithromycin	16	0.125	128X
Erythromycin	32	0.5	64X
Amikacin	16	4	4X
Clindamycin	>64	64	N/A
RNA Polymerase			
Rifampicin	32	2	16X
DNA Gyrase			
Ofloxacin	8	2	4X
Other			
Pyrazinamide	>64	>64	N/A
Pretomanid	>64	>64	" "

925
926

927

Table 2: MIC (µg/ml) of *Mab* Clinical Isolates +/- PBP-lipo knockdown (Cell Wall Antibiotics)

Clinical Isolate	Ampicillin			Amoxicillin			Meropenem	
	-ATc	+ATc		-ATc	+ATc		-ATc	+ATc
ATCC 19977	>256	2		>256	2		128	128
T35	>256	< 0.5		>256	< 0.5		>256	256
T37	>256	< 0.5		>256	< 0.5		>256	256
T49	>256	4		>256	4		>256	128
T50	>256	4		>256	4		>256	128
T51	>256	2		>256	2		>256	256
T53	>256	4		>256	2		>256	256
T56	>256	<0.5		>256	<0.5		>256	128
BWH-B	>256	8		>256	2		>256	256
BWH-C	>256	4		>256	8		>256	256
BWH-E	>256	4		>256	2		>256	256

928
929

930

Table 3: MIC (µg/ml) of *Mab* Clinical Isolates +/- PBP-lipo Knockdown
(Rifampicin and Clarithromycin)

Clinical Isolate	Rifampicin			Clarithromycin	
	-ATc	+ATc		-ATc	+ATc
ATCC 19977	32	2		16	0.125
T35	4	0.25		2	0.25
T37	16	1		2	0.25
T49	64	4		2	0.25
T50	32	1		16	0.25
T51	64	4		16	0.5
T53	32	1		8	0.5
T56	8	1		2	0.25
BWH-B	32	1		16	0.25
BWH-C	32	2		32	1
BWH-E	16	1		16	0.125

931